Results in Engineering 20 (2023) 101404

Contents lists available at ScienceDirect

Results in Engineering

journal homepage: www.sciencedirect.com/journal/results-in-engineering

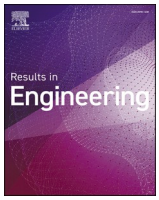

Investigating the potential of using solid waste generated from stone cutting factories for phenol removal from wastewater: A study of adsorption kinetics and isotherms

Nada Al-Ananzeh [a], Khalid Bani-Melhem [b,*], Hussam Elddin Khasawneh [a], Muhammad Tawalbeh [c,d], Zakaria Al-Qodah [e], Ahmad Al-Bodour [f]

[a] Department of Chemical Engineering, Al-Huson University College, Al-Balqa Applied University, Al-Huson P.O. Box 50, Al-Huson, 21510, Jordan
[b] Water Technology Unit (WTU), Center for Advanced Materials (CAM), Qatar University, P.O. Box 2713, Doha, Qatar
[c] Sustainable and Renewable Energy Engineering Department, University of Sharjah, P.O. Box 27272, Sharjah, United Arab Emirates
[d] Sustainable Energy & Power Systems Research Centre, RISE, University of Sharjah, P.O. Box 27272, Sharjah, United Arab Emirates
[e] Chemical Engineering Department, Faculty of Engineering Technology, Al-Balqa Applied University, Marka, P.O. Box 340558, Amman, 11134, Jordan
[f] Chemical and Paper Engineering Department, College of Engineering and Applied Sciences, Western Michigan University, Kalamazoo, MI, 49008-5462, USA

ARTICLE INFO

Keywords:
Solid waste
Stone cutting factories
Wastewater treatment
Phenol removal
Solid characterization
Adsorption
Kinetics and isotherms

ABSTRACT

Remarkably toxic, phenol requires efficient elimination from water. This study investigates the utilization of solid waste generated by stone-cutting factories for extracting phenol from wastewater. The solid waste underwent thermal treatment at 105 °C for 3 h for characterization. Batch adsorption experiments systematically assessed parameters like phenol concentration, adsorbent mass, contact time, temperature, and pH. Optimal removal transpired at pH 7.5, reaching equilibrium within 4 h. Phenol uptake equilibrium values were 8.1, 13.3, 16.2, 20.2, and 28.1 mg/g for initial concentrations of 50, 100, 150, 200, and 300 mg/L, respectively using 1 g of adsorbent at ambient temperature. The Langmuir model fit acceptably, yet the Freundlich model surpassed it. The most suitable kinetics model for phenol adsorption was the pseudo-second-order. The nature of the adsorption process was endothermic. Importantly, this study pioneers the promising application of solid waste generated from stone-cutting factories as an adsorbent material for effective phenol removal, offering a sustainable approach. Notably, no previous study has been conducted on phenol removal from wastewater using this specific adsorbent, rendering this work pivotal in exploring its potential. This solid waste presents an economical, readily available, and environmentally benign material for the adsorption process, expected to exhibit substantial adsorption capacity.

1. Introduction

In the factories dedicated to cutting and shaping stone and granite, a process necessary to meet the high demand for construction materials, substantial pieces of stone extracted from quarries undergo these transformations. Unfortunately, this activity generates significant amounts of waste, comprising solid refuse and sludge. The accumulation of such waste gives rise to notable environmental concerns, poses risks to health, and imposes economic burdens upon the stone-cutting facilities.

To manage this waste, stone factories are compelled to construct sizable reservoirs in which it can be held for up to three weeks before its eventual disposal in sanitary landfills. Both environmental consciousness and prudent waste management practices encourage researchers to explore recycling options, taking into account the pressing environmental and economic factors. Nevertheless, the topic of waste from stone-cutting factories has received limited attention in the existing literature, with most efforts focusing on its incorporation into concrete mixtures, bricks, asphalt, and porcelain materials [1].

Industrial wastewater harbors various types of contaminants, deriving predominantly from industrial activities such as petrochemical, petroleum, pharmaceutical, textile, and resin production. Additional sources include the utilization of chemicals for diverse purposes like disinfection, cleaning, fertilization, detergents, insect extermination, and purification [2–7]. Among the hazardous substances present, phenol is a noteworthy example, possessing carcinogenic properties. In

* Corresponding author..
E-mail addresses: nadaalananzeh@bau.edu.jo (N. Al-Ananzeh), kmelhem@qu.edu.qa (K. Bani-Melhem).

https://doi.org/10.1016/j.rineng.2023.101404
Received 27 July 2023; Received in revised form 28 August 2023; Accepted 5 September 2023
Available online 6 September 2023

wastewater, concentrations of phenol ranging from 12 to 300 mg/L were found in the effluent from resin plants and up to 1000 mg/L in coke processing wastewater [8]. Notably, the maximum allowable phenol concentration in drinking water is set at 0.001 mg/L by the United States Environmental Protection Agency (USEPA) [9,10]. The presence of phenol presents a significant challenge to wastewater treatment, underscoring the importance of its efficient removal from water sources.

Numerous strategies have been explored for the extraction of phenol from wastewater, encompassing liquid-liquid extraction, solar reactors, photocatalytic degradation, steam distillation, biodegradation, oxidation processes, membrane separation techniques, and adsorption [11–17]. Among these, adsorption stands out as a promising and practical solution for phenol removal due to its notable efficiency, cost-effectiveness, and straightforward operational and design attributes compared to other methodologies. The potential of employing activated carbon as an adsorbent for phenol removal has been investigated; however, its relatively high cost has been a drawback [18–20].

In the quest for economical adsorbents for wastewater treatment, a range of materials has been explored, including natural resources and byproducts from agriculture and industry [21–26]. Clays and modified clays, valued for their cost-effectiveness and accessibility, have emerged as potential candidates for pollutant removal [27]. Experiments using inorganic and organic montmorillonites as adsorbents for phenol uptake from wastewater, with initial concentrations ranging from 25 to 175 mg/L, 0.1 g of adsorbent in a 20 mL solution, and a pH of 5, yielded phenol uptakes in the range of 2–14 mg/g [28]. Utilizing calcined magnesium-zinc-aluminum clay at a concentration of 10 g/L and a pH of 7, Tabana et al. achieved a maximum phenol uptake of 12 mg/g [29]. Raw and calcined clays exhibited phenol uptakes of 1.64 and 2.932 mg/g, respectively [30]. Other clays displayed phenol uptakes of 2–18 mg/kg and 0.07–0.33 mmol/g for Modified montmorillonites, as summarized in Table 1. Through the application of modified eggshell powder, Kashi [31] attained a phenol removal rate of 79–92%. Zeolite led to a remarkable 93–100% phenol removal rate in the study conducted by Saravanakumar et al. [32]. Meanwhile, using Chitosan under specified conditions, Meng et al. achieved a phenol uptake ranging from 2 to 36 mg/g [33].

Activated carbon, derived from diverse raw materials, has shown exceptional performance in phenol removal from wastewater, as depicted in Table 1. Notably, activated carbon produced from pomegranate peel achieved a substantial phenol uptake of 148.38 mg/g for initial phenol concentrations ranging from 25 to 175 mg/L [19]. Activated carbon sourced from tea residue exhibited phenol uptakes ranging from 80 to 320 mg/g [20]. In a significant finding, Abdel-Ghani et al. [36] achieved a phenol removal rate of 79–98% by converting African beech wood sawdust into activated carbon for use as an adsorbent. Activated Sugarcane bagasse residues demonstrated phenol uptakes of 2–101 mg/g [8], while coconut shell-based activated carbon removed 23–56 mg of phenol per gram of adsorbent [37].

The objective of this study is to investigate the viability of utilizing solid waste derived from nearby stone cutting factories as an adsorbent for removing phenol from wastewater. Remarkably, as of the current research, no prior investigations have been conducted utilizing this particular adsorbent for phenol removal in wastewater. This solid waste constitutes a cost-effective, abundantly accessible, and environmentally friendly material ideally suited for the adsorption process [32]. Notably, this resource is readily accessible in the northern region of Jordan, particularly in the city of Irbid, where a multitude of stone cutting and shaping facilities are situated, catering to the construction industry's demand for stones and marble.

Table 1
Different adsorbents for phenol uptake from wastewater.

Adsorbent	Phenol uptake	Experimental Conditions	Refs.
Chitosan	2–36 mg/g	20–145 mg/L phenol, pH = 7, 20 mg/25 mL adsorbent, 30–60 °C, 0–3 h.	[33]
Sugarcane bagasse residues	2–101 mg/g for SCBACS 2–46 mg/g for SCBACS	100–1200 mg/L phenol, 2–12 pH, 0.01–0.2 g adsorbent, 17–55 °C, 0–750 min.	[8]
Eggshell powder	79–92% removal with time 50–90% removal with adsorbent mass	5–15 mg/L phenol, 3–11 pH, 3–5 g adsorbent, 20 °C, 0–120 min.	[31]
Raw and calcined clays	2.932 mg/g for calcined clays 1.640 mg/g for raw clays	10–50 mg/L phenol, pH = 4, 0.2 g adsorbent, 20–60 °C, 0–120 min.	[30]
Modified montmorillonites	68% removal 0.07–0.33 mmol/g	0.5 mmol/L phenol, pH = 6, 1.0 g adsorbent, 25–55 °C, 0–120 min.	[34]
Modified montmorillonites	2–18 mg/kg	20–200 mg/L phenol, pH = 7, 0.1–1.5 g adsorbent, 25–45 °C, 0–7 h.	[35]
Inorganic–organic montmorillonites	2–14 mg/g	25–175 mg/L phenol, pH ~ 5, 0.1 g adsorbent, 25–45 °C, 0–7 h.	[28]
Pomegranate peel	148.38 mg/g	25–175 mg/L phenol, pH = 7, 0.1 g adsorbent, 23 °C, 1 h.	[21]
Calcined magnesium-zinc-aluminum layered double hydroxide clay	10–85% removal 12 mg/g	20–200 mg/L phenol, pH = 7, 5–20 g/L adsorbent, 25 °C, 0–24 h.	[29]
Tea residue converted to activated carbon	80–320 mg/g	200–1400 mg/L phenol, pH = 7, 1 g/L adsorbent, 30 °C, 60 min.	[22]
sawdust converted to activated carbon	79–98% removal	5–100 mg/L phenol, pH = 7 (2–10), 0.1–2.5 g/L adsorbent, 25 °C, 300 min.	[36]
Activated carbon from coconut shell	23–56 mg/g	100–400 mg/L phenol, pH = 7, 0.5–1 g/250 mL adsorbent, 25 °C, 0–24 h.	[37]
Zeolite	93–100% removal	100–500 mg/L phenol, pH = 3–9, 0.8–5.2 g/100 mL adsorbent, 25 °C, 0–24 h.	[32]

2. Methods and materials

Fig. 1 shows a schematic diagram of the whole processes conducted in this study. The solid waste used in this study was sourced from a local stone-cutting factory located in Irbid, northern Jordan. To prepare the material, it underwent standard Tyler screen analysis, and the portion passing through a 100-mesh sieve was retained for further use. Subsequently, the solid waste was dried at 105 °C in an electric oven for 3 h to obtain the treated solid waste (TSW).

Several analytical techniques were employed to characterize the TSW. X-ray diffraction (XRD) analysis was conducted using an Ultima VI 185 mm instrument from Rigaku Japan. Particle size and surface area were determined through BET nitrogen surface area measurements using a NOVA 4200e instrument (2–20 nm), following established protocols [2,38]. Scanning electron microscopy (SEM) imaging was employed to assess surface properties, with imaging performed using an FEI QUANTA FEG 450 microscope. The structural composition of the solid waste was further elucidated via Fourier transform infrared spectroscopy (FTIR) utilizing a Bruker VERTEX 8 device, covering a wavelength range of 500–5000 cm^{-1} [39]. All chemicals used were of analytical grade and procured from Sigma-Aldrich.

To create phenol solutions of varying concentrations, a 1000 mg/L stock solution was prepared daily in the laboratory, and the required volumes of deionized water were added accordingly. The removal of phenol was studied under varying conditions, including different time intervals (0–600 min), adsorbent concentrations (1–5 g/L), phenol concentrations (50–300 mg/L), pH levels (4–11), and temperatures

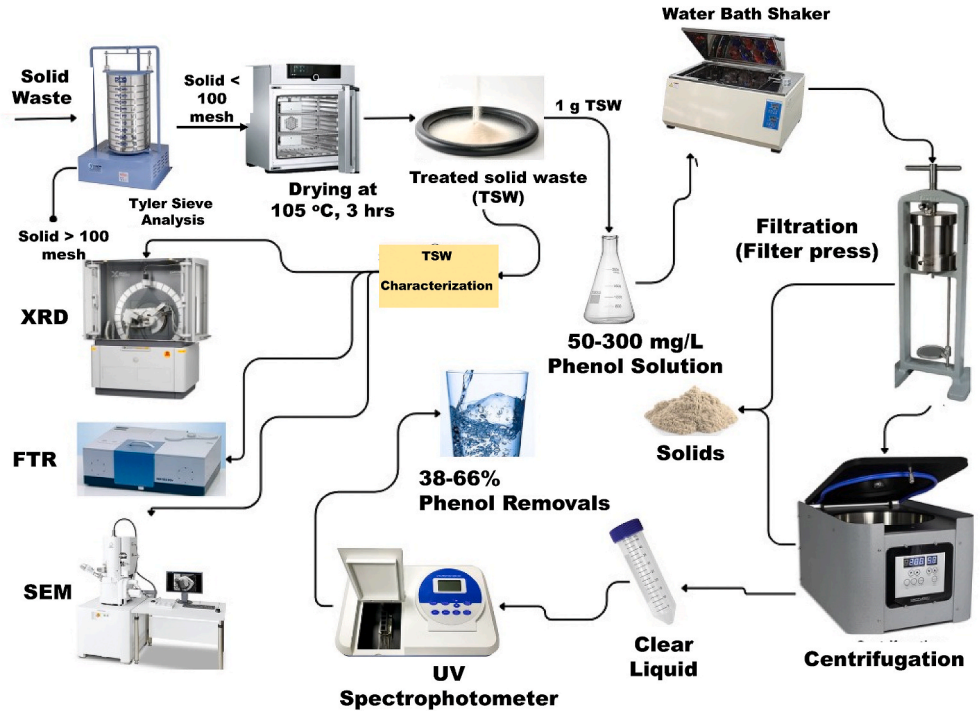

Fig. 1. A schematic diagram of phenol removal using TSW.

(25–45 °C). In each experimental run, initial concentration of phenol was fixed, required mass of TSW was added and pH was adjusted in a 250 glass flask. The mixture was transferred into a water bath shaker (JISICO Water Bath) and mixed at 150 rpm for the desired time period. After each experimental run, samples were subjected to filtration using a Fam filter press 300 series, followed by centrifugation using a Pro-Analytical centrifuge (Centurion Scientific Ltd) to separate solids from the aqueous solution. The phenol concentration in the aqueous solutions was determined using a UV spectrophotometer (JASCO V-730 series) following established standard methods [2,40]. Sodium hydroxide and hydrochloric acid solutions (0.1 N) were utilized to adjust the pH as needed. Each experimental run was conducted in triplicate.

The kinetics, isotherm analysis of phenol adsorption, and the regeneration of spent TSW powder were carried out according to established procedures [2,9]. The TSW demonstrated excellent regeneration potential, with only a slight reduction in adsorption capacity for the regenerated powder.

Phenol percentage removal (Removal efficiency (%)) and phenol uptake or adsorption capacity (q) (mg/g) were determined using Equations (1) and (2), respectively.

$$\text{Removal efficiency } (\%) = \left(\frac{C_0 - C_e}{C_0}\right) \times 100 \quad (1)$$

$$q = (C_0 - C_t) \times \left(\frac{V}{m}\right) \quad (2)$$

where C_o, C_e, and C_t are the concentrations of phenol in mg/L at initial, at equilibrium, and at time t, respectively. V is the volume of the treated solution in L, m is the mass of adsorbent in g, and q is phenol uptake or adsorption capacity in mg/g [41].

3. Results and discussion

3.1. Characterization of the solid waste

Fig. 2 (A) displays the XRD spectrum of the TSW before adsorption. The TSW composition is primarily composed of $CaCO_3$, CaO, and Ca

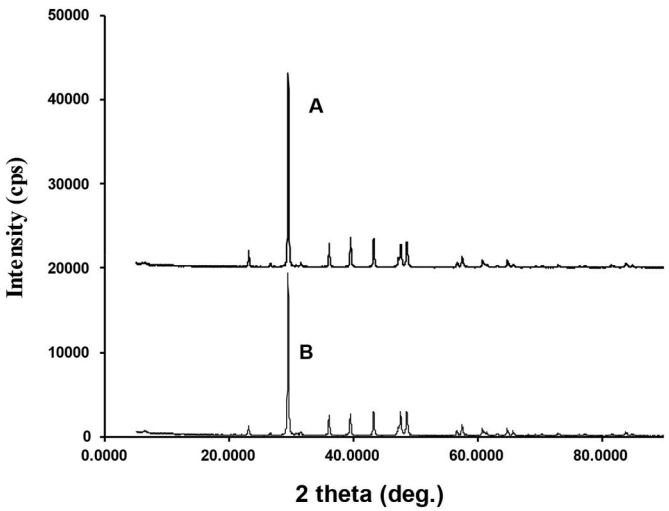

Fig. 2. XRD analysis of TSW (A) before and (B) after adsorption.

$(OH)_2$, as evidenced by the peaks listed in Table 2 [28,42]. Additionally, there are minor peaks observed at 2 theta degrees (2Θ deg.) of 26.5, 60.0, and 66 for Quarts, 23.0 and 46.3 for Kaolinite, 30.7 and 27.8 for feldspar, and 19.9, 34, and 58 for Semicite [30,42]. In Fig. 2 (B), the XRD spectrum of the solid after phenol adsorption at 105 °C is presented. A comparison with Fig. 2 (A) reveals a decrease in peak intensities after phenol adsorption. This decrease can be attributed to the inclusion of phenol within the interfoliar spaces of the solid, and notably, no new peaks emerge in the XRD spectra post-adsorption. These results support the hypothesis of physical phenol adsorption. The solid powder's grain

Table 2
2Θ deg. values from XRD analysis.

Species	CaO	$Ca(OH)_2$	$CaCO_3$
2Θ deg.	32.0, 37.0	29.4, 39.4, 43.2, 53.6	34.0, 47.1, 50.5, 48.8

size ranges from 55 nm to 150 nm, with a particle size of 70 nm determined from BET and SEM analysis, yielding a surface area of 6.1 m^2/g. This value is lower than that reported for raw clays by Quallal et al. [30]. Surface area plays a pivotal role in the adsorption process, as it enhances the adsorption rate [38].

Fig. 3 showcases SEM images of the fresh TSW powder. The surface exhibits irregularities, porosity, roughness, and some agglomerates, resulting in heterogeneous and regular pores that offer a larger surface area for phenol adsorption. Following exposure to a phenol solution, the SEM in Fig. 3 shows a regular adhesive solid surface after phenol adsorption. In Fig. 4 (A), FTIR analysis of the TSW before adsorption reveals bands corresponding to $CaCO_3$ (at 2870, 2357, 1794, 1435, 872, and 711 cm^{-1}) and Si–*O*–Si bonds in Kaolinite or Quartz (at 1035 and 470 cm^{-1}). A water band is evident at 3743 cm^{-1} [18,43,44]. Fig. 4 (B) displays the FTIR study after phenol adsorption, revealing new bands compared to Fig. 4 (A). Bands at 3577, 3549, and 3941 cm^{-1} indicate water hydration of cations and internal OH units of Kaolinite. This arises from phenol adsorption through hydrogen bonding with water molecules in the cation hydration sphere after penetrating the interlayers of the solid (Kaolinite). The band separation below 1345 cm^{-1} suggests the involvement of Si–*O*–Si in the interface with phenol [45,46]. The dispersion of TSW in water exhibits lyophobic colloidal behavior, as supported by XRD and FTIR findings [47]. When sodium chloride is introduced, coagulation occurs. In situations where the solid surface tension is lower than that of the liquid (lyophobic), an increasing contact angle is observed as the solid surface roughness decreases. Initially, liquid droplets reside on the solid surface, gradually being absorbed over time. This phenomenon establishes a relationship between time and evolving contact angles due to ongoing liquid absorption [48,49]. The mass of the adsorbent before and after adsorption showed less than a 3% change in mass. In a leaching test, fresh TSW samples were mixed with deionized water overnight, and no leaching of phenol from the solid into the deionized water was observed, consistent with prior findings [50,51].

3.2. Adsorption results

Phenol adsorption in aqueous solution on the TSW obtained from the waste from a stone cutting factory was examined by optimizing the constraints such as contact time, pH, amount of adsorbent, and the starting concentration of solute.

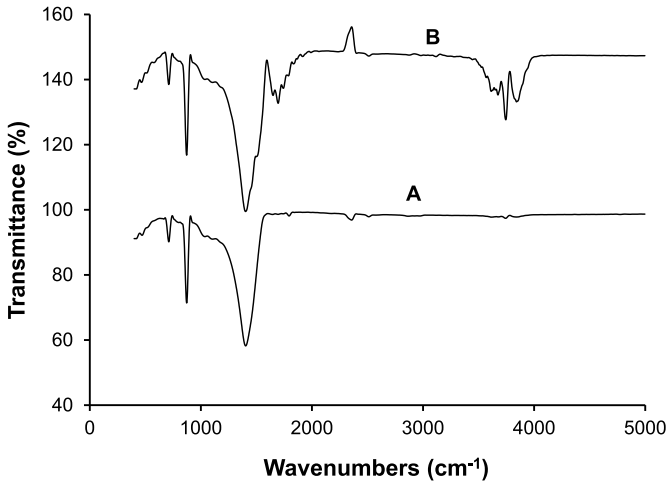

Fig. 4. FTIR analysis of TSW (A) before and (B) after adsorption.

3.2.1. The contact time effect

Fig. 5 illustrates the variations in the percentage (%) removal of phenol (% removal) over different batch runs concerning interaction time. The experimental conditions involved the use of 1 g of TSW in 250 mL of solution at a pH of 7.5, a temperature of 25 °C, and initial phenol concentrations of 50, 100, 150, 200, and 300 mg/L. Phenol removal exhibited a continuous increase as the interaction time progressed until it reached a plateau, marking the equilibrium points, as evident from the results presented in Fig. 5. Based on these outcomes, an interaction time of 200 min was selected as the equilibrium time for the subsequent phases of the study. This behavior can be explained by the initial high solute concentration gradient, the strong affinity of active functional groups for phenol, and the availability of empty and active sites on the solid surface, leading to robust surface binding [30]. As the adsorption process continues over time, the number of available adsorbent sites and the concentration gradient decrease, resulting in a decrease in the rate of phenol adsorption onto the TSW powder.

Furthermore, these findings suggest that phenol molecules form monolayer and multi-layer configurations on the external surface and within the pores of the TSW powder, with pore diffusion occurring on the inner surface of the TSW powder [10]. As the initial phenol

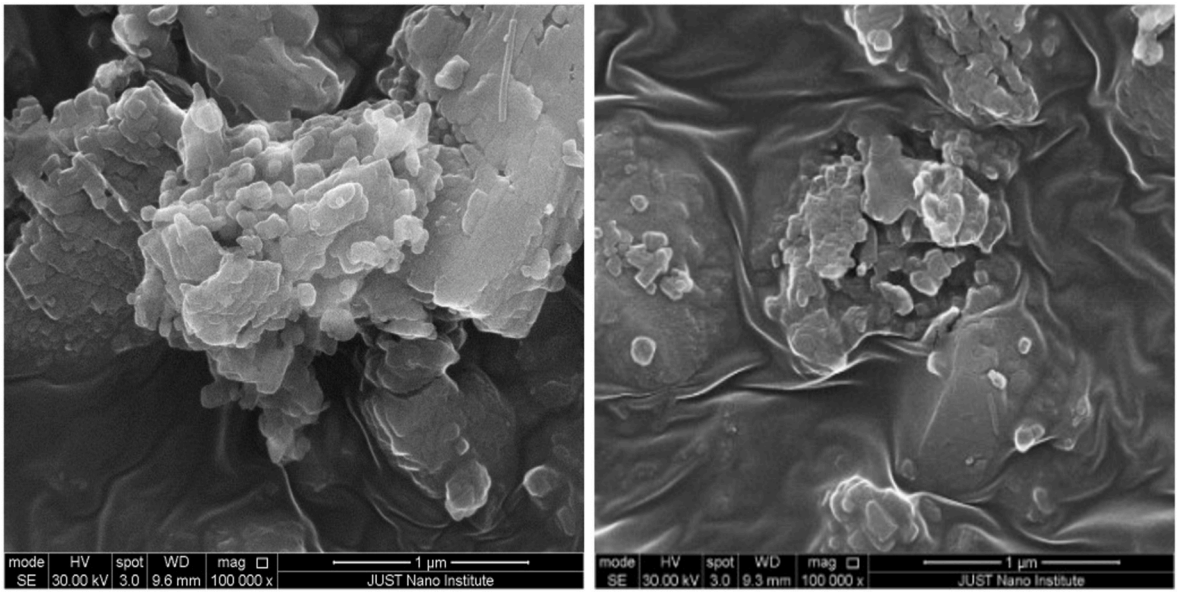

Fig. 3. SEM images of TSW; before adsorption on the left and after adsorption on the right.

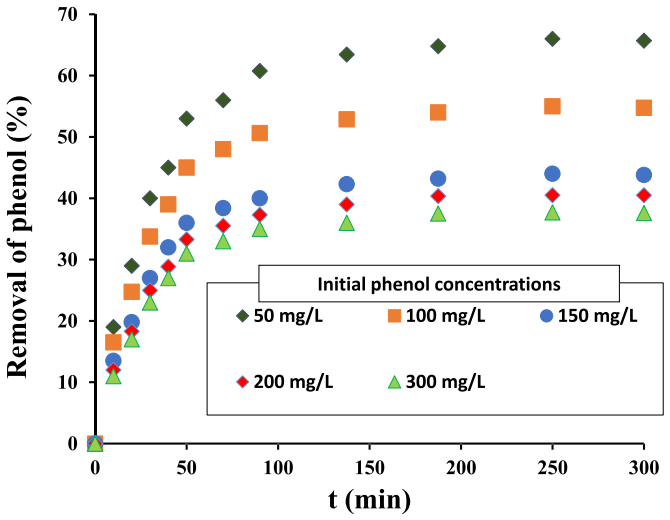

Fig. 5. Effect of contact time on the removal of phenol, 250 mL, pH = 7.5, 1 g of adsorbent and T = 25 °C.

concentration increases from 50 to 300 mg/L, the percentage removal of phenol declines from 65% to 37.6%. This indicates that the rate of phenol removal over time is directly proportional to the phenol ion concentration in the solutions. At higher phenol concentrations, the active sites on the TSW powder become saturated more quickly, resulting in reduced mass transfer of phenol. The increasing initial concentration creates a steeper concentration gradient, enhancing the driving force and consequently improving the initial adsorption rate [52].

3.2.2. *The effect of pH and mass of adsorbent*

The percentage removal of phenol at equilibrium was found at changed pH readings as given in Fig. 6. A slight improvement in the removal of phenol with increasing pH value from 4 to 7.5. After this value pH, phenol removal started to decline. Phenol exits in molecular form in neutral and acidic medium and exits in the ionic state in basic one since the pKa of phenol is 9.89 at 298 K. The increase of OH^- ions in a basic medium increases the difficulty of phenol ions diffusion and increases electrostatic repulsions between the negatively charged particles resulting in a reduction in phenol adsorption. Consequently, the adsorption affinity converts to a lower value in the basic solution. The reduction in phenol removal at the lower pH value is due to the presence of H^+ that competes for the negative active sites on the adsorbent surface [21].

In Fig. 7, the impact of varying the adsorbent mass on phenol removal is depicted, with all other parameters held constant. As the adsorbent mass was adjusted from 0.2 g to 1 g, the equilibrium removal of phenol increased from 25% to 54%. This enhancement can be attributed to the presence of a greater number of active and unoccupied adsorption sites when the adsorbent mass was increased from 0.2 to 1.0 g. However, when the adsorbent mass exceeded 1.0 g, there was a slight reduction in phenol removal. This decrease may be linked to an increase in turbidity, which could hinder the transport of phenol within the solution [53].

3.2.3. *Adsorption kinetics*

The analysis of phenol uptake, q (mg/g) with time applying was performed by applying the pseudo-first order kinetics model and pseudo-second order kinetics model, specified in equations (3) and (4), respectively [54].

$$\log(q_e - q_t) = \log(q_e) - \frac{k_1}{2.303} \times t \tag{3}$$

$$\frac{t}{q_t} = \frac{1}{k_2.q_e^2} + \frac{1}{q_e}t \tag{4}$$

where k_1 and k_2 are the reaction constants of the pseudo-first-order reaction model (min^{-1}) and the pseudo-second-order reaction model (g/mg. min), respectively, q_e is the adsorption capacity at equilibrium (mg/g) and q_t is the adsorption capacity at time t (mg/g). Furthermore, The Weber-Morris intra-particle model given by Eq. (5) was used to further inspect the kinetics of adsorption.

$$q_t = k_d t^{0.5} + C_1 \tag{5}$$

where k_d represents the intra-particle diffusion rate constant (mg/g. $min^{1/2}$) and C_1 is a second constant (mg/g).

Fig. 8 (A) and (B) show the linear fittings of pseudo-first order and pseudo-second order, respectively; while Fig. 8 (C) and (D) represent the fittings of Weber-Morris intra-particle for the whole time zone in the study and when time zone was divided to two zones (Two-zone intra-particle fittings), respectively. On the other hand, Table 3 gives the summary of the linear fittings obtained from kinetic models at various initial concentrations of phenol. The value of the pseudo-second order kinetics rate constant (k_2) reduced from 0.0066 to 0.0018 when the initial concentration of phenol was increased from 50 to 300 mg/L as

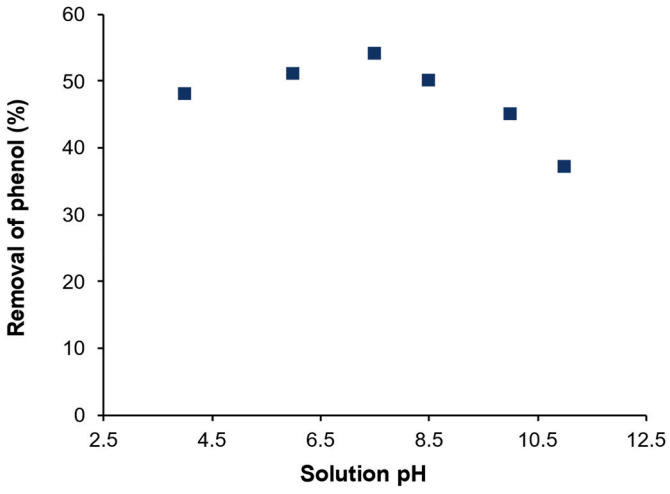

Fig. 6. Effect of pH on phenol removal using TSW with 100 mg/L, 250 mL, 1 g of adsorbent and T = 25 °C.

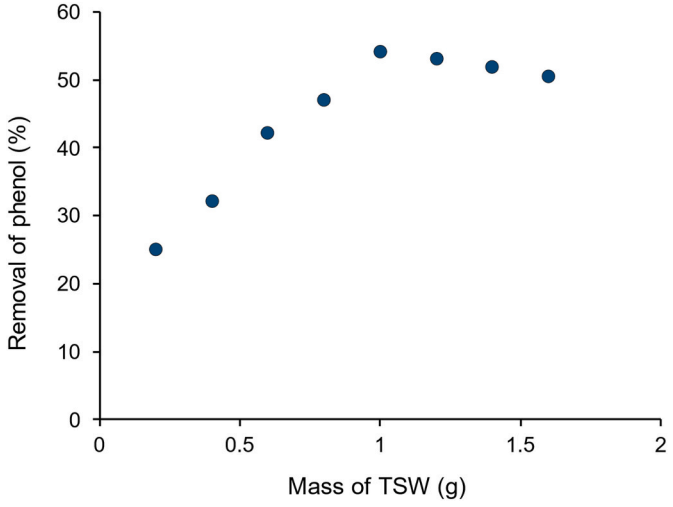

Fig. 7. Effect of mass of TSW on phenol removal with 100 mg/L, 250 mL, T = 25 °C, pH = 7.5.

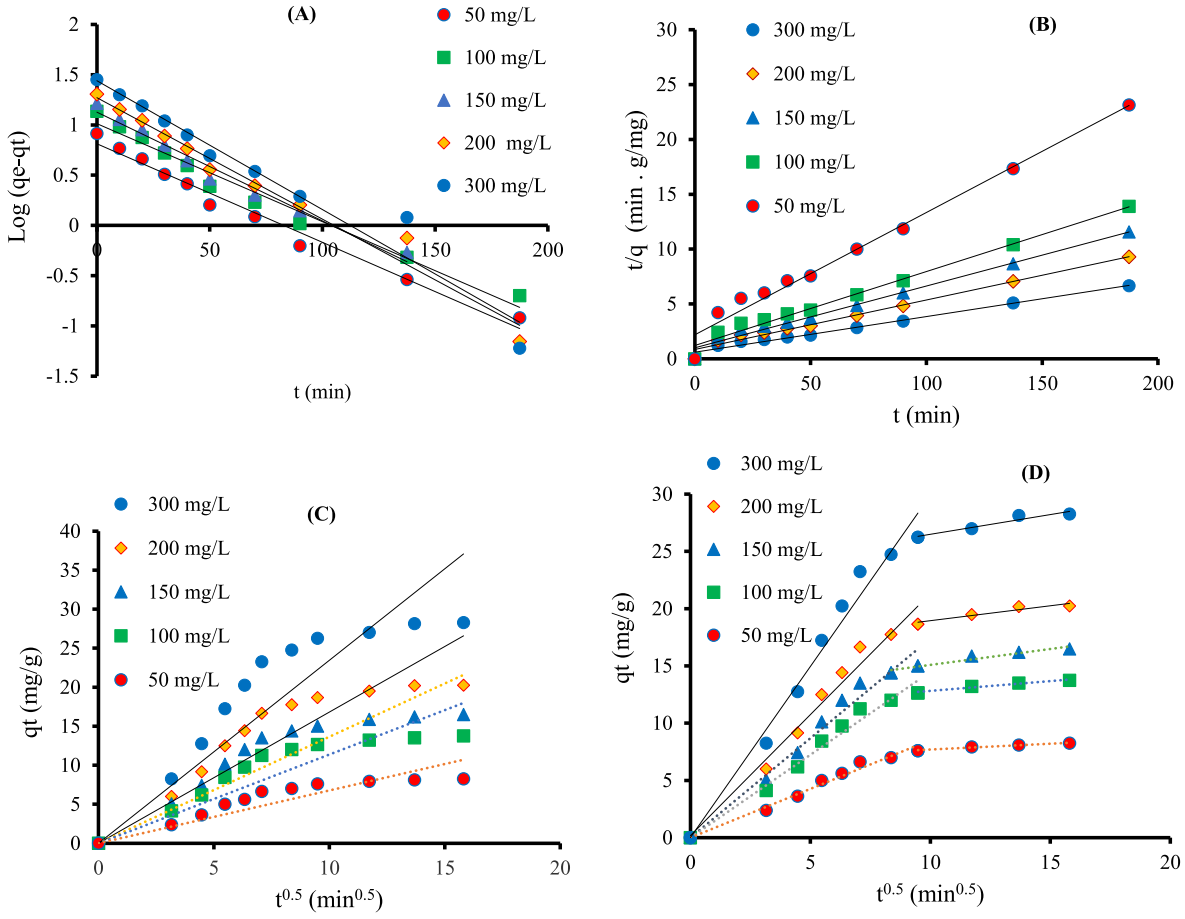

Fig. 8. (A) Pseudo-first order kinetic fittings, (B) Pseudo-second order kinetic fittings, (C) Weber-Morris intra-particle fittings, (D) Two-zone intra-particle fittings. At 1.0 g of adsorbent, 250 mL, T = 25 °C and pH = 7.5.

Table 3
Fitting parameters from kinetic models.

		First order kinetics			Second order kinetics		
Phenol Con. (mg/L)	q_e (Exp.)* (mg/g)	k_1 (1/min)	q_e (Cal.) (mg/g)	R^2	k_2 (g/mg. min)	q_e (Cal.)** (mg/g)	R^2
50	8.10	0.0225	6.62	0.960	0.0066	8.60	0.982
100	13.50	0.0226	10.30	0.970	0.0041	14.8	0.984
150	16.20	0.0249	13.42	0.960	0.0035	17.5	0.985
200	20.18	0.0279	18.70	0.977	0.0021	22.0	0.983
300	28.14	0.0295	27.50	0.956	0.0018	30.0	0.984

* (Exp.) = Experimental value.
** (Cal.) = The value from the fitting results.

can be seen in Table 3. From the obtained readings of second-order rate constants, it can be observed that phenol removal by the adsorbent (TSW) was fastest kinetically at a starting phenol concentration of 50 mg/L. The slower phenol uptake at the higher concentration of phenol could be explained by the mesoporous saturation of the sites on the adsorbent surface with phenol compound leading to a greater resistance during phenols transfer resulting in slower phenol uptake [10].

From the results in Table 3 and, it can be noticed that pseudo-first order and pseudo second order models were able to represent phenol adsorption results with high regression value greater than 0.95. This could indicate that both physical and chemical adsorption processes might be involved [18]. The second order kinetics fit was superior to the other studied simulations as given by the higher R^2 readings shown in Table 3. The value of equilibrium adsorption uptake, q_e (cal.) (mg/g), that is found from the fitting results, is in good agreement with the experimental one, q_e (exp.) (mg/g), for the pseudo-second order kinetics as can be seen in Table 3. The fitting of phenol adsorption results to pseudo-second order kinetics is resolved in the literature for adsorbents [10,34,35]. When adsorption results are well presented by the pseudo-second order kinetics model, this will point to that valence changes through sharing of electrons between adsorbate and the surface of adsorbent is directly related to the rate of adsorption [22].

The model in Eq. (5) helps to understand the mechanism of diffusion. The outcomes from this model simulation are displayed in Fig. 8 (C) and (D). It can be seen from Fig. 8 (C) that the intra particle model fitting was poor (R^2 = 0.6) in fitting the adsorption data. A similar finding was obtained previously when modified montmorillonites was used for phenol removal [35]. However, this model fitted the data better when time was divided into two zones as done in Fig. 8 (D). A first one with a fast rate of adsorption from 0 to 100 min (R^2 = 0.97), then a slower adsorption process from 100 to 240 min (R^2 = 0.9). This would indicate that phenol uptake by TSW is a multi-step process which consists of phenol linkage on the outside surface of TSW followed by internal diffusion of particles that is supported by the excellent fitting of the results with Freundlich model for multi-layer adsorption [2,18].

3.2.4. *Adsorption isotherms and thermodynamics*

Batch adsorption experiments were conducted to analyze the results and investigate the optimal use of the adsorbent. These experiments aimed to determine the adsorbent's capacity, the removal of solute, and

the interaction between the solute and the adsorbent surface. To achieve these objectives, two well-known isotherm models, the multi-layer Freundlich and the single-layer Langmuir, were applied to fit the adsorption data.

The linear forms of the Langmuir and Freundlich isotherm models are expressed in Equations (6) and (7), respectively [2]:

$$\frac{1}{q_e} = \frac{1}{q_{max}} + \frac{1}{q_{max} k_L} \times \frac{1}{C_e} \quad (6)$$

$$\log q_e = \log(k_f) + \frac{1}{n} \times \log(C_e) \quad (7)$$

In these equations, q_e represents the adsorption capacity at equilibrium (mg/g), q_{max} is the maximum adsorption capacity or uptake capacity (mg/g), C_e is the equilibrium concentration (mg/L), k_L is the Langmuir adsorption constant (L/mg), 1/n is the exponent of nonlinearity for the Freundlich model, and k_f is the Freundlich adsorption constant (mg/g).

To gain further insight into the equilibrium behavior, batch adsorption experiments were conducted for 4 h, covering various initial phenol concentrations (50, 100, 150, 200, and 300 mg/L) in 250 mL volumes at a pH of 7.5, using 1 g of TSW at 25 °C. In the specified experimental conditions, the phenol uptake at equilibrium yielded the following results: 8.1, 13.3, 16.2, 20.2, and 28.1 mg/g at 50, 100, 150, 200, and 300 mg/L, respectively. These findings highlight the strong phenol removal capacity by TSW when compared to previous studies outlined in Table 1 mentioned previously.

The results for Freundlich fitting are depicted in Fig. 9 (A), while those for Langmuir are shown in Fig. 9 (B). These figures highlight that both Langmuir and Freundlich isotherms accurately represent the adsorption data, with R^2 values exceeding 0.9. Notably, the Freundlich isotherm exhibits higher regression values, as indicated in Table 4, suggesting a preference for multi-layer adsorption over mono-layer adsorption due to the heterogeneous nature of the solid surface. This finding aligns with the assumption of a heterogeneous surface made in the Freundlich model [9]. Similar observations were reported in other studies focused on phenol adsorption [30]. A summary of the isotherms fitted to the experimental batch adsorption data is provided in Table 4.

Table 4
Isotherms fitting parameters.

Isothermal Model	Parameter	Temperature (°C)			Enthalpy and Entropy
		25	35	45	
Langmuir	q_{max} (mg/g)	27.70	37.59	44.84	
	k_L (L/mg)	0.0229	0.0201	0.0225	
	R^2	0.9670	0.9780	0.9720	ΔH = 4.184 (kJ/mol)
Freundlich	k_f (mg/g)	1.899	2.052	2.145	
	n	1.993	1.802	1.616	ΔS = 0.0330 (kJ/mol.K)
	R^2	0.9822	0.9873	0.9913	
	ln b	0.6413	0.7189	0.7632	
	ΔG (kJ/mol)	- 5.04	- 5.40	- 5.70	

For thermodynamic analysis, batch runs were conducted at temperatures of 25 °C, 35 °C, and 45 °C, as presented in Fig. 9. Utilizing the data from Table 3 and Equation (8) [30]:

$$\ln b = \frac{-\Delta H}{RT} + b_2 \quad (8)$$

where R represents the ideal gas constant (0.008314 kJ/mol·K), b is equal to the equilibrium constant k_f , b_2 ($b_2 = \Delta S/R$) is the energy constant, ΔS is the entropy change (kJ/mol.K), T denotes the temperature in Kelvin (K), and ΔH signifies the heat of reaction (kJ/mol). The plot of ln(b) against 1/T, as illustrated in Fig. 9 (C), yields a ΔH value of 4.184 kJ/mol, indicating a potential endothermic adsorption of phenol

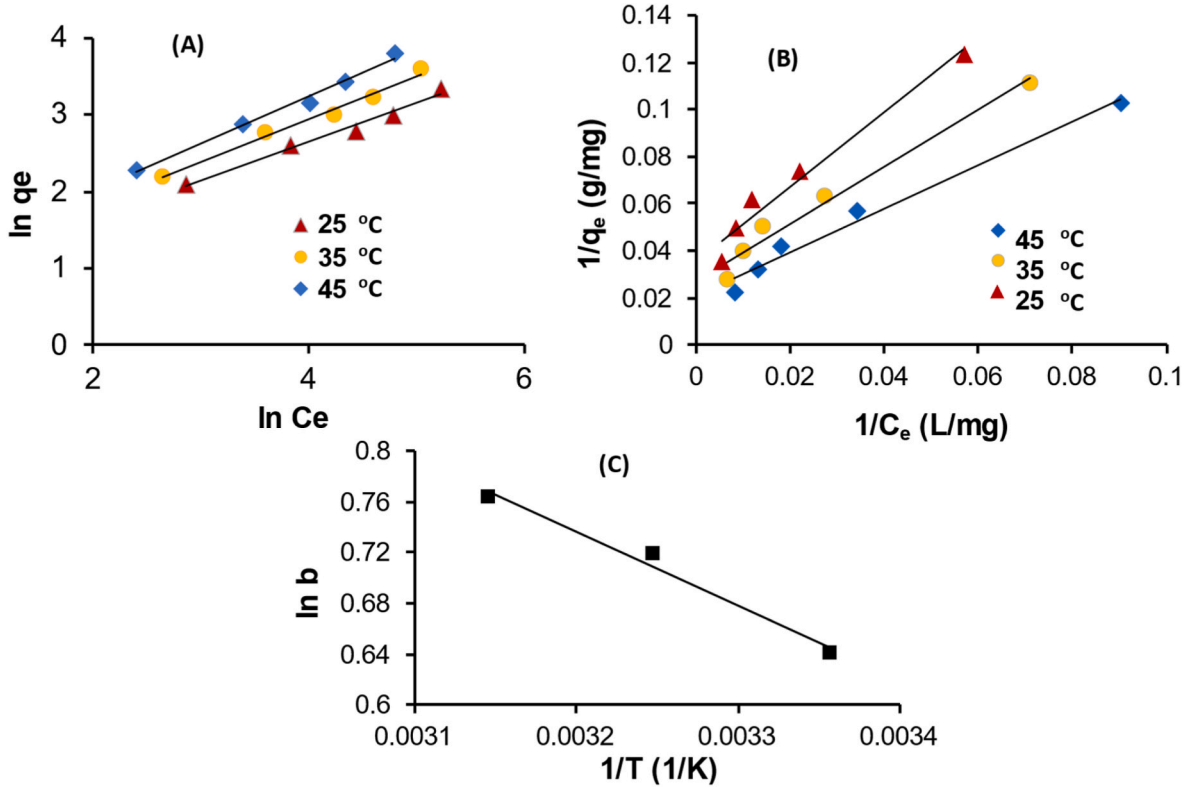

Fig. 9. (A) Freundlich isotherm, (B) Langmuir isotherm and (C)The plot of ln (b) vs. reciprocal of temperature (1/T) for the adsorption phenol with initial phenol concentration: 50, 100, 150, 200, and 300 mg/L, 1.0 g of adsorbent, 250 mL, pH = 7.5. C_e (mg/L), q_e (mg/g).

as the temperature rises from 25 °C to 45 °C. Additionally, this value suggests a low interaction between phenol and the adsorbent surface [22]. Comparable studies have found that phenol uptake by clays and activated sugarcane bagasse residue, as well as oil desulfurization onto nanoporous activated carbon, are endothermic processes [8,30,55]. The improvement in phenol removal with increasing temperature can be attributed to enhanced adsorption forces among the adsorbed species and active sites on the adsorbent [35]. The calculated negative values of Gibbs free energy (ΔG) , $\Delta G = \Delta H - T\Delta S$, confirm the spontaneous and physical nature of the adsorption [28]. Furthermore, the value of R_f, calculated using $R_f = 1/(1 + k_f * C_o)$, is 0.5, indicating favorable adsorption isotherms [10].

4. Conclusions

This study explored the potential of using solid waste produced from a stone-cutting factory as adsorbent material to combat phenol contamination in wastewater. The main adsorbent component was identified as calcium carbonate, accompanied by minor impurities. Phenol removal increased with longer interaction time, peaking at 4 h. Optimal removal occurred at pH 7.5, using 1 g of adsorbent material. Both Langmuir and Freundlich isotherm models fit well with R-squared values above 0.9, favoring the Freundlich model. A thermodynamic investigation confirmed an endothermic adsorption process. The best fit for adsorption kinetics was the pseudo-second-order model. Using stone-cutting factory waste for phenol removal offers promising waste reduction and environmental benefits within the studied parameters. Further research will focus on refining design and optimization possibilities due to the pioneering nature of this study.

Funding

This research did not receive any specific grant from funding agencies in the public, commercial, or not-for-profit sectors.

Declaration of competing interest

The authors declare that they have no known competing financial interests or personal relationships that could have appeared to influence the work reported in this paper

Data availability

Data will be made available on request.

Acknowledgment

Great appreciation for Al-Balqa' Applied University (AAU), Engineer Raeda Tashtosh and for Nanotechnology Center at Jordan University of Science and Technology for performing XRD, SEM and FTIR analysis.

Open Access funding provided by the Qatar National Library.

References

[1] H.A. Mohamadien, The Effect of marble powder and silica fume as partial replacement for cement on mortar, Int. J. Civ. Struct. Eng. 3 (2) (2012) 418–428, https://doi.org/10.6088/ijcser.201203013039.

[2] N.M. Al-Ananzeh, Treatment of wastewater from a dairy plant by adsorption using synthesized copper oxide nanoparticles: kinetics and isotherms modeling optimization, Water Sci. Technol. 83 (7) (2021) 1591–1604, https://doi.org/10.2166/wst.2021.089.

[3] S. Li, B. Qi, J. Luo, Y. Wan, Degradation of phenolic inhibitors by laccase immobilized on tannic acid/polyethylenimine modified magnetic nanoparticles, Results Eng 15 (August) (2022), 100585, https://doi.org/10.1016/j.rineng.2022.100585.

[4] A. Akter, et al., Construction of F-doped Co3O4/Co3O3.69F0.31 nanocomposite for boosting photocatalytic removal of organics from industrial waste H2O under visible-light, Results Eng 16 (August) (2022), 100672, https://doi.org/10.1016/j.rineng.2022.100672.

[5] P.O. Oladoye, T.O. Ajiboye, E.O. Omotola, O.J. Oyewola, Methylene blue dye: toxicity and potential elimination technology from wastewater, Results Eng 16 (September) (2022), 100678, https://doi.org/10.1016/j.rineng.2022.100678.

[6] N.S. Ali, H.N. Harharah, I.K. Salih, N.M. Cata Saady, S. Zendehboudi, T. M. Albayati, Applying MCM-48 mesoporous material, equilibrium, isotherm, and mechanism for the effective adsorption of 4-nitroaniline from wastewater, Sci. Rep. 13 (1) (2023) 1–15, https://doi.org/10.1038/s41598-023-37090-4.

[7] N.S. Ali, K.R. Kalash, A.N. Ahmed, T.M. Albayati, Performance of a solar photocatalysis reactor as pretreatment for wastewater via UV, UV/TiO2, and UV/H2O2 to control membrane fouling, Sci. Rep. 12 (1) (2022) 1–10, https://doi.org/10.1038/s41598-022-20984-0.

[8] M.A. Akl, Efficient removal of phenol from water samples using sugarcane bagasse based activated carbon, J. Anal. Bioanal. Tech. 5 (2) (2014), https://doi.org/10.4172/2155-9872.1000189.

[9] N.M. Al-Ananzeh, Bio-adsorption of phenol from wastewater applying local jordanian eucalyptus leaves: parametric, kinetics, adsorption isotherms, and surface analysis, Desalination Water Treat. 223 (2021) 180–187, https://doi.org/10.5004/dwt.2021.27126.

[10] S. Ho, Low-cost adsorbents for the removal of phenol/phenolics, pesticides, and dyes from wastewater systems: a review, Water (Switzerland) 14 (20) (2022), https://doi.org/10.3390/w14203203.

[11] M.F. Abid, O.N. Abdulla, A.F. Kadhim, Study on removal of phenol from synthetic wastewater using solar photo catalytic reactor, J. King Saud Univ. - Eng. Sci. 31 (2) (Apr. 2019) 131–139, https://doi.org/10.1016/j.jksues.2017.03.002.

[12] A.K. Behera, K.P. Shadangi, P.K. Sarangi, Synthesis of dye-sensitized TiO2/Ag doped nano-composites using UV photoreduction process for phenol degradation: a comparative study, Environ. Pollut. 312 (Nov. 2022), 120019, https://doi.org/10.1016/J.ENVPOL.2022.120019.

[13] S. Jaber, et al., Biodegradation of phenol and catechol in cloud water: comparison to chemical oxidation in the atmospheric multiphase system, Atmos. Chem. Phys. 20 (8) (Apr. 2020) 4987–4997, https://doi.org/10.5194/acp-20-4987-2020.

[14] W. Raza, J. Lee, N. Raza, Y. Luo, K.-H. Kim, J. Yang, Removal of phenolic compounds from industrial waste water based on membrane-based technologies, J. Ind. Eng. Chem. 71 (Mar. 2019) 1–18, https://doi.org/10.1016/j.jiec.2018.11.024.

[15] Y.A. Ahmed, R.H. Salman, Simultaneous electrodeposition of multicomponent of Mn–Co–Ni oxides electrodes for phenol removal by anodic oxidation, Case Stud. Chem. Environ. Eng. 8 (May) (2023), 100386, https://doi.org/10.1016/j.cscee.2023.100386.

[16] N. Aryanti, A. Nafiunisa, V.F. Giraldi, L. Buchori, Separation of organic compounds and metal ions by micellar-enhanced ultrafiltration using plant-based natural surfactant (saponin), Case Stud. Chem. Environ. Eng. 8 (May) (2023), 100367, https://doi.org/10.1016/j.cscee.2023.100367.

[17] S.V. Manjunath, B.R. Yakshith, M. Meghashree, Synergistic analysis for co-treatment of poultry wastewater and sewage in electro-chemical system: operational parameters, kinetics and energy estimation, Results Eng 19 (April) (2023), 101275, https://doi.org/10.1016/j.rineng.2023.101275.

[18] Y. Dehmani, D. Dridi, T. Lamhasni, S. Abouarnadasse, R. Chtourou, E.C. Lima, Review of phenol adsorption on transition metal oxides and other adsorbents, J. Water Process Eng. 49 (Oct. 2022), 102965, https://doi.org/10.1016/j.jwpe.2022.102965.

[19] A.A.Q. Al-Qadri, Q.A. Drmosh, S.A. Onaizi, Enhancement of bisphenol a removal from wastewater via the covalent functionalization of graphene oxide with short amine molecules, Case Stud. Chem. Environ. Eng. 6 (July) (2022), 100233, https://doi.org/10.1016/j.cscee.2022.100233.

[20] Z.T. Chong, L.S. Soh, W.F. Yong, Valorization of agriculture wastes as biosorbents for adsorption of emerging pollutants: modification, remediation and industry application, Results Eng 17 (December 2022) (2023), 100960, https://doi.org/10.1016/j.rineng.2023.100960.

[21] M. Afsharnia, M. Saeidi, A. Zarei, M.R. Narooie, H. Biglari, Phenol removal from aqueous environment by adsorption onto pomegranate peel carbon, Electron. Physician 8 (11) (Nov. 2016) 3248–3256, https://doi.org/10.19082/3248.

[22] J. Tao, P. Huo, Z. Fu, J. Zhang, Z. Yang, D. Zhang, Characterization and phenol adsorption performance of activated carbon prepared from tea residue by NaOH activation, Environ. Technol. (United Kingdom) 40 (2) (2019) 171–181, https://doi.org/10.1080/09593330.2017.1384069.

[23] C. Alex Mbachu, A. Kamoru Babayemi, T. Chinedu Egbosiuba, J. Ifeanyichukwu Ike, I. Jacinta Ani, S. Mustapha, Green synthesis of iron oxide nanoparticles by Taguchi design of experiment method for effective adsorption of methylene blue and methyl orange from textile wastewater, Results Eng. 19 (March) (2023), 101198, https://doi.org/10.1016/j.rineng.2023.101198.

[24] W.G. Djonga, E. Noubissié, G.B. Noumi, Discoloration test of a slaughterhouse effluent by adsorption on two adsorbents produced from sawdust of Khaya senegalensis and Pinus sp, Results Eng. 4 (November) (2019), https://doi.org/10.1016/j.rineng.2019.100068.

[25] Z. Guisela B, D.A. Ohana N, D. Dalvani S, V. Fermin G, L. Francisco HM, N.G. Luis, Adsorption of arsenic anions in water using modified lignocellulosic adsorbents, Results Eng. 13 (January) (2022), https://doi.org/10.1016/j.rineng.2022.100340.

[26] N. Madkhali, et al., Recent update on photocatalytic degradation of pollutants in waste water using TiO2-based heterostructured materials, Results Eng. 17 (October 2022) (2023), 100920, https://doi.org/10.1016/j.rineng.2023.100920.

[27] X. Hu, et al., Effect of double carbon chains on enhanced removal of phenol from wastewater by amphoteric-gemini complex-modified bentonite, Environ. Pollut. 320 (2023), 121088, https://doi.org/10.1016/J.ENVPOL.2023.121088.

[28] L. Ma, et al., Adsorption of phenol, phosphate and Cd(II) by inorganic-organic montmorillonites: a comparative study of single and multiple solute, Colloids

Surfaces A Physicochem. Eng. Asp. 497 (Ii) (2016) 63–71, https://doi.org/10.1016/j.colsurfa.2016.02.032.
[29] L. Tabana, S. Tichapondwa, F. Labuschagne, E. Chirwa, Adsorption of phenol fromwastewater using calcined magnesium-zinc-aluminium layered double hydroxide clay, Sustain. Times 12 (10) (2020), https://doi.org/10.3390/su12104273.
[30] H. Ouallal, Y. Dehmani, H. Moussout, L. Messaoudi, M. Azrour, M.A.H. Ouallal, Y. Dehmani, H. Moussout, L. Messaoudi, Kinetic, isotherm and mechanism investigations of the removal of phenols from water by raw and calcined clays, Heliyon 5 (5) (2019), e01616, https://doi.org/10.1016/j.heliyon.2019.e01616.
[31] K. Kashi, On the analysis of phenol removal from drinking water by batch reactor using powdered eggshell Giti, Biosci. Biotechnol. Res. Commun. 10 (2) (2017) 276–286, https://doi.org/10.21786/bbrc/10.2/47.
[32] K. Saravanakumar, A. Kumar, Removal of phenol from aqueous solution by adsorption using zeolite, Afr. J. Agric. Res. 8 (23) (2013) 2965–2969, https://doi.org/10.5897/AJAR11.194.
[33] J.M. Li, X.G. Meng, C.W. Hu, J. Du, Adsorption of phenol, p-chlorophenol and p-nitrophenol onto functional chitosan, Bioresour. Technol. 100 (3) (2009) 1168–1173, https://doi.org/10.1016/j.biortech.2008.09.015.
[34] Z. Luo, M. Gao, S. Yang, Q. Yang, Adsorption of phenols on reduced-charge montmorillonites modified by bispyridinium dibromides: mechanism, kinetics and thermodynamics studies, Colloids Surfaces A Physicochem. Eng. Asp. 482 (2015) 222–230, https://doi.org/10.1016/j.colsurfa.2015.05.014.
[35] Y. Li, et al., Adsorption behavior of phenol by reversible surfactant-modified montmorillonite: mechanism, thermodynamics, and regeneration, Chem. Eng. J. 334 (2018) 1214–1221, https://doi.org/10.1016/j.cej.2017.09.140.
[36] N.T. Abdel-Ghani, G.A. El-Chaghaby, F.S. Helal, Preparation, characterization and phenol adsorption capacity of activated carbons from African beech wood sawdust, Glob. J. Environ. Sci. Manag. 2 (3) (2016) 209–222, https://doi.org/10.7508/gjesm.2016.03.001.
[37] M.S. Ripa, R. Mahmood, S. Khan, E.A. Khan, Adsorption of phenol from aqueous solution using activated carbon prepared from coconut shell, J. Chem. Eng. 29 (1) (2017) 9–13, https://doi.org/10.3329/jce.v29i1.33812.
[38] N.S. Ali, et al., Modification of SBA-15 mesoporous silica as an active heterogeneous catalyst for the hydroisomerization and hydrocracking of n-heptane, Heliyon 8 (6) (2022), e09737, https://doi.org/10.1016/j.heliyon.2022.e09737.
[39] N.S. Abbood, N.S. Ali, E.H. Khader, H.S. Majdi, T.M. Albayati, N.M.C. Saady, Photocatalytic degradation of cefotaxime pharmaceutical compounds onto a modified nanocatalyst, Res. Chem. Intermed. 49 (1) (2023) 43–56, https://doi.org/10.1007/s11164-022-04879-3.
[40] H.J. Al-Jaaf, N.S. Ali, S.M. Alardhi, T.M. Albayati, Implementing eggplant peels as an efficient bio-adsorbent for treatment of oily domestic wastewater, Desalination Water Treat. 245 (2022) 226–237, https://doi.org/10.5004/dwt.2022.27986.
[41] N.N. Bahrudin, M.A. Nawi, Lelifajri, Kinetics and isotherm modeling of phenol adsorption by immobilizable activated carbon, React. Kinet. Mech. Catal. 126 (1) (Feb. 2019) 61–82, https://doi.org/10.1007/s11144-018-01528-y.
[42] R. Molinder, T.P. Comyn, N. Hondow, J.E. Parker, V. Dupont, In situ X-ray diffraction of CaO based CO2 sorbents, Energy Environ. Sci. 5 (10) (2012) 8958, https://doi.org/10.1039/c2ee21779a.
[43] J. Ojima, Determining of crystalline silica in respirable dust samples by infrared spectrophotometry in the presence of interferences, J. Occup. Health 45 (2) (2003) 94–103, https://doi.org/10.1539/joh.45.94.
[44] J. Kikouama, K. Konan, A. Katty, J. Bonnet, L. Balde, N. Yagoubi, Physicochemical characterization of edible clays and release of trace elements, Appl. Clay Sci. 43 (1) (2009) 135–141, https://doi.org/10.1016/j.clay.2008.07.031.
[45] J. Madejová, FTIR techniques in clay mineral studies, Vib. Spectrosc. 31 (1) (2003) 1–10, https://doi.org/10.1016/S0924-2031(02)00065-6.
[46] A. Tabak, B. Afsin, S.F. Aygun, E. Koksal, Structural characteristics of organo-modified bentonites of different origin, J. Therm. Anal. Calorim. 87 (2) (2007) 377–382, https://doi.org/10.1007/s10973-006-7886-6.
[47] W.E. W, Clay and CeramicS Raw Material : second ed., vol. 4, Elsivier Applied Science Publishers LTD, London and NewYork, 1986.
[48] M. Seibold, A, M. Nardin, J. Schultz, A. Walliser, Oppliger, Effect of dynamic contact angle on capillary rise phenomena, Colloids Surfaces A Physicochem. Eng. Asp. 161 (2000) 81–87.
[49] W. A, G.A. Adamson, Physical Chemistry of Surfaces, sixth ed., John Wiley & Sons, NewYork, 1997.
[50] W.A. Muslim, S.K. Al-Nasri, T.M. Albayati, Evaluation of Bentonite, attapulgite, and kaolinite as eco-friendly adsorbents in the treatment of real radioactive wastewater containing Cs-137, Prog. Nucl. Energy 162 (2023), 104730, https://doi.org/10.1016/j.pnucene.2023.104730.
[51] C. Vipulanandan, Effect of clays and cement on the solidification/stabilization of phenol-contaminated soils, Waste Manag. 15 (5–6) (1995) 399–406, https://doi.org/10.1016/0956-053X(95)00041-W.
[52] S. Lakshmi, M. Harshitha, G. Vaishalia, S. Keerthana, R. Muthappa, Studies on different methods for removal of phenol in waste water - review, Int. J. Sci. Eng. Technol. Res. 5 (7) (2016) 2288–2496.
[53] M.R. Mohammad, A.H. Afaj, M.N. Mahmoud, Study of some effecting factors on the removal of phenol from aqueous solutions by adsorption onto activated carbon, J. Int. Environ. Appl. Sci. 11 (2) (2016) 148–153.
[54] D. Choque-Quispe, et al., Multimetal removal in aqueous medium using a potato starch/nopal mucilage copolymer: a study of adsorption kinetics and isotherms, Results Eng. 18 (March) (2023), https://doi.org/10.1016/j.rineng.2023.101164.
[55] T. Al-Khodor, A.A. Y, Albayati, Real heavy crude oil desulfurization onto nanoporous activated carbon implementing batch adsorption process: equilibrium, kinetics, and thermodynamic studies, Chem. Africa 6 (2023) 747–756, https://doi.org/10.1007/s42250-022-00482-6.